Feasibility Study of $LiSiH_3$ as Hydrogen Storage Material

By

Tuhin Shaikh
18201005
Audrey Orpean Hossain
20111002

A thesis submitted to the Department of Mathematics and Natural Science in partial fulfillment of the requirements for the degree of B.Sc. in Physics

Department of Mathematics and Natural Sciences
BRAC University

Declaration

1. The thesis submitted is our own original work while completing our degree at BRAC University.
2. The thesis does not contain material previously published or written by a third party, except where this is appropriately cited through full and accurate referencing.
3. The thesis does not contain material which has been accepted, or submitted, for any other degree or diploma at a university or other institution.
4. We have acknowledged all main sources of help.

Student's Full Name & Signature:

Tuhin Shaikh	**Audrey Orpean Hossain**
ID: 18201005	ID: 20111002

Approval

The thesis titled ”Feasibility study of $LiSiH_3$ as Hydrogen Storage”, submitted by Tuhin Shaikh (ID: 18201005) and Audrey Orpean Hossain (ID: 20111002), has been accepted as satisfactory in partial fulfilment of the requirements for the degree of Bachelor of Science in Physics on 20 November 2025.

Examining Committee:

Supervisor: **(Member)**	Md. Firoze Haque Associate Professor and chairperson, Department of Mathematics and Natural Science BRAC University
Co-Supervisor: **(Member)**	Muhammad Lutfor Rahman Assistant Professor, Department of Mathematics and Natural Science BRAC University

Program Coordinator:
(Member)

Muhammad Lutfor Rahman
Assistant Professor,
Department of Mathematics
and Natural Science
BRAC University

Departmental Head:
(Chair)

Md. Firoze Haque
Associate Professor,
Department of Mathematics
and Natural Science
BRAC University

Ethics Statement

To the best of my knowledge, this study presents the first theoretical exploration of $LiSiH_3$ as a hydrogen storage material. $LiSiH_3$ demonstrates remarkable stability, efficient hydrogen absorption and desorption, and favorable electronic properties, including its band structure and conductivity, making it a promising candidate for sustainable energy storage.

I declare that there are no competing financial interests or personal relationships that could have influenced the findings of this thesis.

Abstract

Solid state hydrogen storage materials must simultaneously satisfy both gravimetric, volumetric, and stability requirements to be viable for onboard energy applications. In this work, first principles density functional theory (DFT) calculations are employed to investigate the structural, electronic, mechanical, thermodynamic and dynamical properties of the complex hydride $LiSiH_3$ as a candidate hydrogen storage medium. From the crystal structure indicate a gravimetric capacity of about 7.9 wt% H_2 ($\approx$2.7 kWh kg^{-1}) and a volumetric energy density of $\approx$4.6 kWh L^{-1}, substantially exceeding the 2025 U.S. Department of Energy targets and outperforming compressed hydrogen at 700 bar. Electronic band structure and projected density of states analyses reveal strong Si–H covalent bonding and a largely ionic interaction between Li^+ and the SiH_3^- framework, consistent with a lightweight, hydrogen rich lattice. Elastic constants satisfy the Born criteria, confirming mechanical stability, although the calculated Pugh's ratio and Poisson's ratio indicate intrinsically brittle behaviour. Thermodynamic functions from the quasi harmonic Debye model approach the classical limits at high temperature, while phonon dispersion curves exhibit pronounced imaginary modes, signalling dynamical instability of the studied phase at ambient conditions. Overall, $LiSiH_3$ offers highly attractive storage capacities

Dedication

In humble gratitude, we dedicate this thesis to the boundless mysteries of the Universe, whose beauty, complexity, and everlasting wonder make the pursuit of knowledge both meaningful and enjoyable.

We would also like to dedicate this thesis to our parents, who've worked so hard to make sure we can be here; to our friends, who've supported our endeavours through thick and thin; and to our teachers, who've given their all to our education.

Acknowledgment

We are profoundly grateful to Almighty Allah for granting us the resilience, courage, and patience needed to complete this research.
We extend our heartfelt appreciation to our supervisors, Dr. Firoze Haque, Muhammad Lutfor Rahman, Senior Researcher Dholon Kumar Paul, whose invaluable guidance, timely support, and thoughtful feedback shaped every stage of this project. Despite their busy schedules, they always made time for our questions and provided continuous encouragement.
We would also like to express our sincere gratitude to the faculty members of the School of Mathematics and Natural Sciences, BRAC University, for their constant support, motivation, and academic guidance. Our special thanks go to Senior Researcher Dholon Kumar Paul, Shahnil Zulkarnain for their mentorship and insightful suggestions.

Contents

List of Figures

List of Acronyms

DFT Density Functional Theory

GGA Generalized Gradient Approximation

LDA Local Density Approximation

CASTEP Cambridge Serial Total Energy Package

DOS Density of States

TDOS Total Density of States

PDOS Partial Density of States

SCF Self Consistent Field

PBE Perdew Burke Ernzerhof

HF Hartree Fock

HEG Homogeneous Electron Gas

DOE Department of Energy

Chapter 1

Introduction

1.1 Background

Hydrogen, recognized as one of the most promising candidates for clean energy storage, faces significant challenges related to its storage and transport [1]. Among the various materials investigated for hydrogen storage, light metal hydrides have garnered attention due to their high hydrogen volumetric density and favorable thermodynamic properties [2]. Lithium silicon hydride ($LiSiH_3$) is one such material that has emerged as a potential candidate for hydrogen storage. $LiSiH_3$, a novel hydride material, is a combination of lithium and silicon with promising hydrogen-binding properties, making it a subject of increasing interest for researchers in the field of energy storage systems [3].

$LiSiH_3$ stands out as a potentially high capacity hydrogen storage material due to its unique structural characteristics and high gravimetric

hydrogen density [4]. The material's ability to release hydrogen at relatively moderate temperatures further enhances its applicability for practical energy storage solutions [5]. Unlike conventional metal hydrides, which often suffer from instability or high temperature requirements for hydrogen release, $LiSiH_3$ offers a potentially safer and more efficient method for hydrogen storage [6].

Despite its promising characteristics, the feasibility of $LiSiH_3$ as a practical hydrogen storage material is not yet fully understood. Key areas requiring further research include its structural stability, hydrogen release kinetics, and material behavior under varying pressure and temperature conditions [7]. Additionally, the impact of doping, alloying, or other modifications on the properties of $LiSiH_3$ for hydrogen storage also warrants investigation [8].

This research aims to assess the feasibility of $LiSiH_3$ as a hydrogen storage material by conducting a detailed study of its structural, mechanical, and thermodynamic properties using first-principles calculations [9]. The findings of this study could provide valuable insights into the potential for $LiSiH_3$ to meet the hydrogen storage demands of future energy systems [10].

1.2 Objectives of the Present Study

The primary objective of this study is to evaluate the feasibility of $LiSiH_3$ as a hydrogen storage material. Specifically, the research will focus on the following objectives:

- **Structural Characteristics**: Investigate the atomic structure and crystal properties of $LiSiH_3$, including its stability and how it changes under different conditions (pressure and temperature).

- **Mechanical Properties**: Examine the mechanical behavior of $LiSiH_3$, including properties such as bulk modulus, shear modulus, and Young's modulus, which are essential for understanding its durability and performance under stress.

- **Thermodynamic Properties**: Analyze the hydrogen storage capacity and release mechanisms, including hydrogen binding energy, desorption temperature, and the material's behavior under varying pressure conditions.

- **Electronic Properties**: Study the electronic structure of $LiSiH_3$, including its band gap and electronic states, to better understand the material's conductive and insulating properties.

- **Hydrogen Storage Feasibility**: Evaluate the potential of $LiSiH_3$ to serve as an effective hydrogen storage material by analyzing the interactions between hydrogen and the material, including the material's ability to reversibly absorb and release hydrogen at practical temperatures and pressures.

1.3 Outline of the Thesis

This thesis is structured as follows:

- **Chapter 1: Introduction** This chapter analysed the the Background why we choose $LiSiH_3$ as hydrogen storage also provided present day study This chapter
- **Chapter 2: Literature Review** This chapter reviews key research on hydrogen storage materials, focusing on metal hydrides and highlighting the role of $LiSiH_3$ in the field, along with its advantages and challenges.
- **Chapter 3: Theoretical Methodology** The computational methods used, including Density Functional Theory (DFT) and simulation techniques, are explained to study the structural, mechanical, and thermodynamic properties of $LiSiH_3$.
- **Chapter 4: Results and Discussion** Computational results on $LiSiH_3$'s hydrogen storage performance are presented, compared with other hydrides, and discussed in terms of practical relevance.
- **Chapter 5: Conclusion and Future Work** The findings are summarized, study limitations are noted, and recommendations for future research on $LiSiH_3$ in hydrogen storage are provided.

.

Chapter 2

Literature Review

2.1 Introduction to Hydrogen Storage

Over the past decade, the development of advanced hydrogen-storage materials has emerged as a critical research direction in the pursuit of a clean and sustainable energy infrastructure. Driven by global efforts to transition away from carbonintensive fuels, researchers have focused extensively on solid state hydrogen storage systems that combine safety, reversibility, and high gravimetric capacity. A broad spectrum of materials including porous adsorbents, metal hydrides, and complex hydrides has been examined under varying thermodynamic and mechanical conditions to evaluate their potential for integration into hydrogen based energy technologies.

Fundamental distinctions exist between physical and chemical hydrogen-storage mechanisms. Physical storage materials rely primarily on physisorption, where hydrogen molecules interact weakly with sur-

faces via van der Waals forces, leading to reversible but typically low energy adsorption processes [11]. Such physisorptive systems depend strongly on surface area and pore morphology, and their performance often diminishes at ambient temperatures due to weak adsorption enthalpies. Chemical storage systems, on the other hand, incorporate hydrogen through stronger bonding interactions. Among these, metal hydrides have been recognized as technologically significant due to their ability to absorb hydrogen directly into the host crystal lattice [12]. These materials have been applied in fields such as neutron moderation, electrochemical cycling, hydrogen purification, and thermal storage, highlighting their versatility and industrial value. Beyond simple hydrides, complex hydrides composed of lightweight cations and polyatomic anions exhibit even higher hydrogen capacities and tunable thermodynamic properties, making them promising candidates for next generation hydrogen storage applications [13].

2.2 $LiSiH_3$ as a Hydrogen Storage Material

Within this broad landscape of hydrogen storage materials, $LiSiH_3$ (lithium silane) has emerged as a promising candidate due to its unique chemical structure, which combines both ionic and covalent bonding. $LiSiH_3$ benefits from the low atomic mass of its constituent elements (Li and Si), which contributes to a high gravimetric hydrogen storage capacity. First principles calculations have demonstrated

that $LiSiH_3$ exhibits not only favorable thermodynamic properties but also mechanical stability under pressure, which is crucial for practical applications [14, 15]. These computational studies suggest that $LiSiH_3$ could be a viable material for hydrogen storage, with high storage densities approaching those of metal hydrides like MgH_2. Furthermore, theoretical models predict that the material's hydrogen desorption temperature could be tuned to match the operational requirements of fuel cells and other hydrogen-based technologies.

However, despite these promising results, experimental data on $LiSiH_3$ remain limited. Much of the research conducted on this material has been theoretical, with only a handful of experimental studies corroborating the computational predictions. The theoretical studies are varied, with differences in computational methods, pseudopotentials, and the treatment of pressure conditions. Thus, while computational studies show promising potential for $LiSiH_3$ as a hydrogen-storage material, more experimental work is required to validate these predictions and optimize the material for real world applications [16].

In line with these developments, lightweight hydride-based frameworks incorporating elements such as lithium, silicon, and hydrogen have attracted growing attention as potential solid state hydrogen carriers. Among them, $LiSiH_3$ has emerged as a particularly interesting candidate due to its mixed ionic covalent bonding character, structural stability, and the inherently low atomic mass of its constituent elements. Preliminary computational studies indicate that $LiSiH_3$ may exhibit favorable hydrogen-storage characteristics, in-

cluding competitive gravimetric density and mechanical tunability under pressure. Despite these promising indications, experimental data remain sparse, and theoretical results show notable variation depending on computational approach, pseudopotential selection, and pressure conditions.

Given these considerations, it is essential to integrate insights from both experimental trends and first principles simulations to evaluate the viability of $LiSiH_3$ as a hydrogen storage material. This section synthesizes current knowledge on hydrogen-storage mechanisms, reviews the computational landscape relevant to hydride based materials, and identifies research gaps that motivate the in depth analysis conducted in subsequent chapters.

2.3 Fundamental Characteristics of Crystals

A crystalline solid is characterized by longn range order and a periodic arrangement of its constituent atoms. The smallest repeating unit, known as the unit cell, defines the lattice through translational symmetry. The geometry of the unit cell is described by lattice parameters such as edge lengths and angles, as well as symmetry elements, which dictate the material's overall structure. These structural properties have a profound influence on the material's electronic, optical, and mechanical properties, as well as its hydrogen storage capacity [17].

In the case of $LiSiH_3$, the crystal structure plays a critical role in

determining its potential for hydrogen storage. As a hydride, the material's lattice structure provides specific sites for hydrogen atoms to occupy. The periodic arrangement of lithium, silicon, and hydrogen atoms forms a regular structure that influences the efficiency of hydrogen absorption and desorption. The lattice parameters of $LiSiH_3$,which include unit cell volume, edge lengths, and bond angles,directly affect its ability to store hydrogen. For instance, a larger unit cell volume may provide more interstitial space for hydrogen atoms, while specific bonding motifs, such as covalent interactions between lithium and silicon atoms, may facilitate more efficient hydrogen absorption.

The crystal structure of $LiSiH_3$ consists of a unique interplay between ionic and covalent bonding. This gives the material both stability and flexibility, making it a promising candidate for reversible hydrogen storage. Furthermore, the nature of these bonds influences the mechanical behavior of the material, such as its response to external pressures, which is important for tuning the material's hydrogen desorption temperature. The geometry of the unit cell also impacts the material's optical properties, which can be leveraged to optimize hydrogen storage under varying conditions.

Thus, understanding the fundamental characteristics of $LiSiH_3$'s crystal structure, including its lattice parameters and symmetry, is essential for predicting its hydrogen storage capabilities. This chapter aims to provide a comprehensive overview of the crystal structure of $LiSiH_3$, along with the theoretical framework used to explore its

mechanical, optical, and hydrogen storage properties.

2.4 Crystal Structure of $LiSiH_3$

2.4.1 Unit Cell

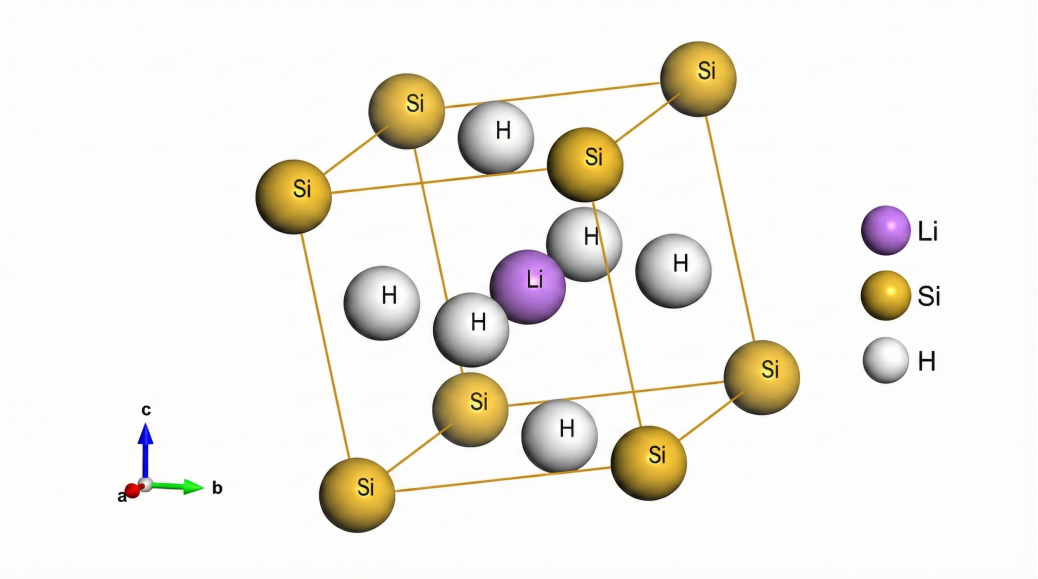

Figure 2.1: Crystal structure of $LiSiH_3$ showing Si (yellow) at the corners, Li (purple) at the body center, and H atoms (grey) occupying the face centered positions.

$LiSiH_3$ crystallizes in a highly symmetric structure belonging to the $Pm\bar{3}m$ (No. 221) space group, which corresponds to the archetypal cubic perovskite arrangement. Within this unit cell, each atom occupies a distinct Wyckoff position with well defined fractional coordinates. Silicon (Si) atoms reside at the 1a Wyckoff site, located at the cube corners with fractional coordinates (0, 0, 0). Lithium

(Li) occupies the 1b Wyckoff site, positioned at the body center of the unit cell with coordinates (0.5, 0.5, 0.5). The three hydrogen (H) atoms populate the 3c Wyckoff positions at (0.5, 0, 0), (0, 0.5, 0), and (0, 0, 0.5), forming a symmetric octahedral environment around the silicon atom.

The arrangement of SiH_6 octahedra connected through corner sharing geometry, combined with the centrally placed Li atom, creates a stable and highly ordered three dimensional framework. This perovskite like atomic configuration is characterized by a balance of ionic interactions (Li–H) and covalent bonding (Si–H), which is particularly favorable for reversible hydrogen storage. The crystal structure of $LiSiH_3$, visualized using Matarial stdio, is presented in Figure 2.1.

2.4.2 Lattice Parameters

The lattice parameters define the geometric dimensions of a three-dimensional crystal lattice, described by the three cell edge lengths a, b, and c, and the three interaxial angles α, β, and γ. In $LiSiH_3$, geometry optimization using CASTEP revealed that the optimized structure maintains equal lattice constants and right angles, confirming a cubic configuration despite being treated under a triclinic lattice framework during computation.

2.4.3 Unit Cell Volume

For a cubic cell, the volume is simply $V = a^3$. Using the optimized lattice constant $a = 3.335974$ Å, the unit cell volume is computed as:

$$V = (3.335974)^3 = 37.125\,\text{Å}^3$$

This volume provides a measure of the space available for hydrogen atoms within the structure.

2.5 Hydrogen Storage Mechanisms in $LiSiH_3$

Hydrogen storage in solids generally follows two mechanisms: physisorption and chemisorption. Physisorption stores H_2 molecules on the surface of porous materials through weak van der Waals forces; the storage capacity depends strongly on surface area and pore volume and diminishes at ambient temperatures [18]. Chemisorption, in contrast, involves dissociative adsorption in which H_2 molecules break into atomic hydrogen and form stronger chemical bonds with the host lattice. Metal hydrides such as $LiSiH_3$ store hydrogen via chemisorption hydrogen atoms occupy interstitial sites or form anions (H^-) that bond with silicon and lithium. This mechanism enables high volumetric storage densities but often requires heat to release hydrogen.

2.6 Criteria for an Ideal Hydrogen Storage Material

An ideal hydrogen storage material must satisfy several key criteria:

- **High gravimetric and volumetric capacities**: A material should store ≥ 7 wt% hydrogen and provide sufficient volumetric density to meet energy requirements for mobile applications.
- **Moderate binding enthalpy**: An enthalpy of absorption in the range of 20–40 kJ mol^{-1} allows reversible hydrogen uptake and release near ambient temperature.
- **Fast kinetics**: Rapid absorption and desorption are necessary to deliver usable hydrogen on demand.
- **Structural stability**: The material must withstand repeated hydrogenation cycles without significant degradation or loss of capacity.
- **Elemental abundance and safety**: Constituent elements should be abundant, non-toxic, and environmentally benign to facilitate large-scale deployment.

These criteria guide the screening of candidate materials and are referenced throughout this work.

2.7 Hydrogen Storage Potential of $LiSiH_3$

First-principles calculations indicate that $LiSiH_3$ is among the most promising members of the $MSiH_3$ hydride family (M = Li, Na, K, Mg) for hydrogen storage. The gravimetric hydrogen storage capacity is predicted to be around 7.9 wt%, surpassing related perovskite hydrides. Calculated formation enthalpies and desorption energies suggest that hydrogen release from $LiSiH_3$ occurs at moderate temperatures, consistent with the criteria outlined in Section 2.6. The mixed ionic covalent bonding character of $LiSiH_3$ allows for reversible hydrogen uptake without severe structural collapse, making it a promising candidate for further investigation.

Chapter 3

Research Methodology

3.1 Classification of Methodology

The academic community has focused a great deal of effort in recent years on computer-based theoretical simulations to identify the different characteristics of materials in the fields of Chemistry and Physics [18, 19]. Analytical investigations may not always yield the same results as computer-based theoretical computations, so to investigate the material's structure and determine its different characteristics, a number of techniques are employed. Three distinct types of methodologies may be identified: (i) the ab-initio or first principles method; (ii) the semi-empirical or empirical method; and (iii) the method of molecular mechanics.

Methods based on ab initio or first principles do not need empirical data to be computed. The values of a few key parameters and the principles of quantum physics are the main sources of dependence

for the ab-initio procedures. For calculating small molecular systems, ab initio approaches may yield extremely precise results. Semi empirical approaches, on the other hand, can perform calculations for macro molecules with less accuracy and require empirical data obtained through experimentation in order to simplify the calculations. Molecular mechanics techniques apply classical physics to the study of atom and molecular dynamics.

This chapter mostly describes the ab-initio procedures. The first principles or ab initio approaches are helpful in forecasting the characteristics of novel materials. For example, they may be used to calculate the energy levels of solid state electrons, as indicated by their energy bands, being the fundamental theoretical challenge in the solid state of physics. Previously, the attainable size of systems for ab-initio approaches were severely limited. Nevertheless, the issue with the aforementioned two approaches has been that, in the absence of computers, the sheer amount of integrals that need to be assessed renders them unfeasible on actual systems [20].

The ability to accurately calculate energies and related properties for systems with up to twelve atoms, including the heaviest elements in the periodic table, in just a mere few minutes is made possible by the remarkable advancement of low-cost, powerful computers. Unlike previously mentioned techniques, ab initio computations can yield excellent quantitative predictions over a wide range of the system. Thus, in order to study structural, electrical, optical, and mechanical characteristics, calculations were carried out throughout this research

using an ab-initio plane wave pseudopotential approach inside the DFT framework employing GGA as used in CASTEP code [21]. This chapter provides an in depth discussion of the complex mathematical processes involved in the ab initio approaches.

3.2 The Wave Function

The probability of a particle quantum state as a function of time, position, momentum, and spin is expressed as a wave function. To represent the wave function, the symbol Ψ is used. In quantum physics, the wave function is an expression in mathematics that is used to characterize a particle system or quantum state. A wave function is simply described as one that explains the qualities of a wave and satisfies the wave equation [22]. A probability function being a real number, is represented by the symbol $|\Psi|^2$, whereas a wave function is a complex number where locating the particle at a specific location and time has a probability of $|\Psi|^2$.

For instance, the wave function of an electron fully describes the behavior of the electron in an atom with a lone electron, like a hydrogen or an ionized helium. The temporal evolution of a wave function is explained by the Schrödinger equation and the rules of quantum physics. As a mathematical form of wave equation, the Schrödinger equation causes the wave function to behave qualitatively like other waves, such as waves on a string or in water. This leads to wave-particle duality and defines the term wave function.

3.3 The Schrödinger Equation

The fundamental equation in physics used to analyze quantum mechanical activity is the Schrödinger equation. This partial differential equation, which describes the evolution of a physical system's wave function over time, is referred to by Schrödinger's wave equation. To find the energy levels of quantum mechanical systems, one applies the Schrödinger equation. The time independent and the time dependent Schrödinger equations are two separate equations that are generally referred to as the Schrödinger equation. The time independent Schrödinger equation is the foundation of both the wave function mechanics and the DFT (density functional theory) [23].

$$\hat{H}\Psi = E\Psi \tag{3.1}$$

Where the total energy, E, of the system and $\hat{H}$ is the Hamiltonian operator that acts on Ψ to provide its eigenvalue. Other operators are accessible as well, such as spin and electric dipole moments. For the physical observables, these may be utilized to get the wave function's expectation values. The Schrödinger equation is challenging to solve for non hydrogenic systems without approximations, despite its apparent simplicity [23, 24].

The Born Oppenheimer (BO) approximation is the fundamental approximation which separates the motion of the system's electrons from that of its nuclei. According to the Born Oppenheimer ap-

proximation, any modification to the nuclei's positions results in an instantaneous restructuring of the electronic configuration; in other words, the nuclei are seen as fixed with regard to the motion of electrons at any geometry, making it easier to assess the interactions between the nuclei and the nuclear kinetic energy, the electron nucleus, and the nucleus nucleus. An interpretation of the approximation is that when the nuclei move, electrons immediately realign because of the enormous mass differential between them and the nucleus.

$$(H_{el} + V_N)\Psi = E_{el}\psi_{el} \tag{3.2}$$

$$H_{el} = T_s + V_{en} + V_{es} \tag{3.3}$$

The nuclear nuclear interactions (V_N) and the electronic interactions (H_{el}) make up the operators in the electronic Schrödinger equation. In the above equation, H_e is made up of the electrons' kinetic energy, T_s; electron-electron potential energy, V_{ei}; and electron nuclear potential energy, V_{es}. The BO approximation states that V_N is a constant at every geometry, therefore it may be inserted as a parameter and subtracted from the equation. Almost all quantum chemistry programs solve the electronic Schrödinger equation.

3.4 Pseudopotentials

A pseudopotential is built with the core radius, r_c, so that it demonstrates symmetry with the actual potential outside of that radius. The ab initio method is used to build the pseudopotential. The purpose of the pseudopotential is to provide an effective potential, or pseudopotential [25], for the non valence electrons in an atom with its nucleus in place of the Columbic potential factor, which is generally contained in the Schrödinger equation. This enables for a modified effective potential term to be included in the equation instead of the Columbic potential term.

Beyond this distance, each pseudo wave function has to align with the appropriate true wavefunction. It is also necessary for the charge densities obtained outside of the core area to match the actual charge density. As a result, over the core region, the integral of the squared amplitudes of the actual and pseudo wave functions must match. Norm conservation is the name given to this circumstance [26]. Phase shifts during scattering over the core must be retained, along with all other atomic characteristics of the element. Since these phase shifts will vary depending on the angular momentum state, the pseudopotential must generally be non local and have projectors for the different angular momentum components.

Hans Hellmann initially presented the pseudopotential approximation in the 1930s. Using a plane wave basis set, the computational complexity would still be prohibitive even if every electron in the

system were explicitly included in the calculation and built from the whole Columbic potential of the nucleus. Due to the extremely high potential in the area and the orthogonality requirement between various states, the wavefunctions close to the nucleus oscillate quickly, necessitating the need for a very large cut off energy and basis set. Thankfully, research in physics and chemistry demonstrates that only valence electrons significantly engage in atomic interactions, with core electrons on distinct atoms being independent of their surroundings. As a result, it is possible to assume that the core electron states are stable and to create a pseudopotential for each atomic species that accounts for the interactions between the nucleus and core electrons. The two forms of pseudopotentials are distinguished by:

- Norm-conserving Pseudopotential
- Ultra-soft Pseudopotential

The calculated and applied norm-conserving pseudopotentials in DFT allow for accurate and efficient ab initio electronic structure computations of intricate polyatomic systems. The following properties are occupied by these pseudopotentials:

- The core atomic states are assumed to be frozen because the majority of the valence electrons determine the majority of the atomic states' physical and chemical characteristics. The term "frozen-core approximation" refers to this.

3.5 Ab-initio Methods

One type of theoretical approach makes use of the atoms' atomic number and the values of basic constants to compute molecular structures and other crystal characteristics without the need for empirical data is called the ab-initio method. The phrase ab initio, obtained from Latin, is formed from the words ab from and initio, derived from initium beginning. When doing ab initio calculations, several numerical operations are needed, and with the increase in size of the molecule or atom, the processing time grows quickly. The ability to accurately compute the characteristics of both tiny and big molecules has been made possible by advances in computing power, and this type of technique may now replace the semi empirical method.

For a range of molecular geometries, the total energy of the molecule may be determined through the ab-initio calculations, and the conformation with the lowest energy are used to determine the bond angles and lengths of the molecules [27]. Ab-initio approaches are able to converge to the precise solution when approximations are small enough in magnitude. However, there is no monotonic convergence, and for some attributes, the most minute calculation may yield the best result. The ab initio approach is used to calculate the chemical and physical characteristics of any periodic system with a particular crystalline structure and chemical composition as accurately as possible [28], without requiring a priori knowledge .

The ab-initio techniques that are most popular are:

- The Hartree Fock method
- The Density Functional Theory (DFT) method

3.5.1 Hartree-Fock Method

A variational method called the Hartree Fock method yields the wave function of a many body quantum system, which for fermions is often expressed as a Slater determinant. An approximation approach for determining the ground state energy and wave function of a quantum many body system is the Hartree Fock (HF) method. Many quantum chemistry issues are addressed using this approach, which was first suggested by Hartree in 1928 [29] and then improved by Fock and Slater in 1930 by integrating the Pauli principle. However, the method is often applied in the matrix formulation provided in 1951, by Roothaan [30].

The method is broken down into multiple steps. Initially the HF equations are made up using the Slater determinant for an electronic configuration. The Fock operator is defined, along with the secular equation; it is iteratively solved until self consistency is achieved. This makes it possible to find a ground tate energy minimum.

The Schrödinger equation of molecules, atoms and solids is often solved using the Hartree Fock technique, although nuclear physics has made extensive use of it. This article's remaining sections will be devoted to electronic structure theory applications. The HF technique makes the assumption that a single Slater determinant (if fermion

particles) or a single permanent (if boson particles) of N spin orbitals may approximate the system's precise, N body wave function. A set of N coupled equations for the N spin orbitals can be obtained by applying the variational principle. These equations may be solved to obtain the approximate values of the system's energy and HF wave function.

The exchange energy is precisely calculated using the HF approach, however the effect of electron correlation is not calculated. It is exceedingly challenging to compute the correlation energy. This is due to the fact that the correlation energy has a direct relationship with the Hilbert space's degrees of freedom, which the single determinant is unable to cover. The vast majority of the wave function approaches include the vacant HF one electron orbitals in this expansion and include several Slater determinants in an attempt to travel across the Hilbert space. Providing a precise representation of the entire electrical wave function would be the main objective.

A 3N dimensional function of complex nature with N spin coordinates makes up the wavefunction in the Born-Oppenheimer approximation, where N being the amount of electrons. For small systems, the computing cost of the multi faceted research for such a wavefunction is practically unsustainable. This being the reason for the DFT analysis, the self consistent field technique is another name for the Hartree Fock approach.

The generated non linear equations' solutions act as though every particle was rendered to the mean-field that every other particle has

formed. An iterative fixed point type approach is used to solve the equations, where this solution strategy is not the only one that may be used, nor is it a necessary component of the HF approach. The electronic characteristics that depend on the crystal's electronic structure are of interest to us. It depends on the electric charge and the geometry of the nuclei, which are assumed to be fixed and organized in a crystalline lattice.

Selecting a Hamiltonian is the first crucial step in any ab-initio investigation of electrical structure. Typically, a crystal is made up of 10^{23} atoms organized in an orderly pattern. Calculating the wavefunction requires consideration of each nucleus and each electron. This wavefunction represents the all inclusive many body wavefunction that fully characterizes the system.

For this wavefunction, the time independent Schrödinger equation will look like this:

$$H\Psi = E\Psi \tag{3.4}$$

$$\left[-\frac{\hbar^2}{2m}\sum_{i=1}^{N_{el}}\nabla_i^2-\frac{\hbar^2}{2}\sum_{i=1}^{N_{at}}\frac{\nabla_i^2}{M_i}-\frac{e^2}{4\pi\varepsilon_0}\frac{1}{2}\sum_{i,j=1}^{N_{el}N_{at}}\frac{Z_j}{|r_i-R_j|}+\right.$$
$$\left.\frac{e^2}{4\pi\varepsilon_0}\frac{1}{2}\sum_{i,j=1}^{N_{at}N_{at}}\frac{Z_iZ_j}{|R_i-R_j|}+\frac{e^2}{4\pi\varepsilon_0}\frac{1}{2}\sum_{i,j=1}^{N_{el}N_{el}}\frac{1}{|r_i-r_j|}\right]$$
$$\Psi(r_1S_1,\ldots r_{N_{el}}S_{N_{el}};R_1,\ldots R_{N_{at}})=E\Psi(r_1S_1,\ldots r_{N_{el}}S_{N_{el}};R_1,\ldots R_{N_{at}}) \tag{3.5}$$

where the atomic number is denoted by Z, M being the atomic mass, and m is the electronic mass; R is the radius vector for the atom and r is the radius vector for the electron. The all inclusive many body wave function Ψ, with energy E has atoms (N_{at}) and electrons (N_{el}). The kinetic expression of the electrons and nuclei are the left hand side's first two terms; the electron nucleus exchange is the third term, the nucleus nucleus component is the fourth, and the electron electron transfer is the fifth [32].

This problem continues to get extensive and complex, thus requiring approximations. The Born Oppenheimer approximation should be performed first. This implies that the mobility of the nuclei is ignored, and the second part in the equation can be taken to be equal to zero. Actually, if the lattice constant is kept unchanged, the nucleus nucleus component will stay unchanged and be equal to zero. In the second, the many body wavefunction is transformed into a collection of decoupled wavefunctions by using the Pauli principle. This may

be accomplished by expressing the entire wavefunction as a Slater determinant of one electron wavefunctions. An approximation to the entire wavefunction is what a Slater determinant is. The ansatz will appear as:

$$\Psi(r_1 s_1, \ldots r_N s_N) = \frac{1}{\sqrt{N!}} \begin{vmatrix} \Psi_1(r_1 s_1) & \Psi_1(r_2 s_2) & \cdots & \Psi_1(r_N s_N) \\ \vdots & \vdots & & \vdots \\ \Psi_N(r_1 s_1) & \Psi_N(r_2 s_2) & \cdots & \Psi_N(r_N s_N) \end{vmatrix} \tag{3.6}$$

where the initial electron wave function at position r_1 with spin s_1 is represented by $\Psi_1(r_1 s_1)$. The electron electron component is separated into two parts using this ansatz, and the resulting set of one electron equations is known as the Hartree Fock equations:

$$\begin{aligned} &\frac{\hbar^2}{2m}\nabla_i^2\psi_i(r,s) - \frac{e^2}{4\pi\varepsilon_0}\left(\frac{1}{2}\right)\sum_{j=1}^{N_{at}}\frac{Z_j}{|r-R_j|}\psi_i(r,s) \\ &\qquad + \sum_{j=1}^{N_{el}}\frac{e^2}{4\pi\varepsilon_0}\int \rho(r')\left(\frac{1}{|r-r'|}\right)dr'\psi_i(r,s) \\ &-\sum_{j=1}^{N_{el}}\frac{1}{4\pi\varepsilon_0}\int \frac{e^2}{|r-r'|}\psi_j^*(r',s_j)\psi_i(r',s_i)\psi_j(r,s_j)\delta_{s_i s_j}dr' = \varepsilon_i\psi_i(r,s) \end{aligned} \tag{3.7}$$

where the Kronecker delta is represented by $\delta_{s_i s_j}$ and the electron density by $\rho(r')$. The electron electron interaction term, which

is divided into the direct term and the exchange term, is the final two terms on the left side of this equation. The Coulomb fields of every other electron are combined in the direct term to form an average field that the electron travels through. The Slater determinant ansatz also satisfies the Pauli principle, which states that the exchange term appears as a result of the anti summarization of the entire wavefunction.

A trial wavefunction for the potential is necessary before the energy can be computed since HF theory implies that an electron moves in a potential that is the average of the potentials owing to all other electrons and nuclei. The Schrödinger equation is then solved repeatedly in order to determine the ideal wavefunction. It implies that a new wavefunction is computed by estimating the wavefunction in the potential terms [32]. The process is then repeated until there is no difference between the old and new wave functions. First, the new wavefunction is used to compute new potential terms. Once this is completed, the Schrödinger equation has an approximate, self consistent solution.

In condensed matter physics, the characteristics of each system are determined by its ground state electronic structure (GSES). Therefore, the primary goals of our attention are the computation of ground state energy and certain other aspects related to energy. As one Slater determinant is insufficient to extend the complete Hilbert space of a set of fully interacting fermions, the Hartree Fock energy is not the proper ground state energy.

Chemists define the so called correlation energy as the difference between the total ground state energy and the Hartree Fock energy:

$$E_c^{che} = E_{total} - E_{HF} \tag{3.8}$$

The exchange energy is precisely calculated using the Hartree Fock technique, but the influence of electron correlation is not calculated at all. Calculating the correlation energy is an extremely challenging task. This is due to the fact that the correlation energy has a direct relationship with the Hilbert space's degrees of freedom, which the single determinant is unable to cover. By adding numerous Slater determinants and including the unoccupied Hartree Fock one electron orbitals in this expansion, most wavefunction approaches attempt to bridge the Hilbert space. To provide an accurate depiction of the entire electrical wavefunction is the aim of this. Here N is the number of electrons, and the Born Oppenheimer approximation is a wavefunction in the 3N dimensional complex function with N spin coordinates. For even relatively tiny systems, the computing cost for the pursuit of a multi dimensional wavefunction is unsustainable. This is the goal of studying density functional theory.

3.5.2 Density Functional Theory

Hohenberg and Kohn [33] devised the DFT. When it comes to explaining the ground state characteristics of insulators, semiconductors, and metals, DFT is a very effective theory as shown by Kohn

and Sham [34]. The fundamental idea behind the DFT is to use density rather than the many-body wave function to explain an interacting system of electrons. An alternative to the ab initio procedure is the DFT. The electronic structure of many body systems, including molecules, atoms, and condensed phases, as well as electron density that are spatially dependent, are described using this technique, which is based on quantum mechanics.

The main objective of DFT is to characterize a dynamic system of fermions using density rather than the many body wave function [35]. N electrons in a solid follow the Pauli principle, which causes them to separate from one another via the Coulomb potential. This suggests that rather than depending on all 3N degrees of freedom, the system's fundamental variable is dependent on three spatial coordinates: x, y, and z. The computational method that Kohn and Sham (KS) presented in the years that followed serves as the basis for DFT [37], as well as two theorems established in 1964, by Hohenberg and Kohn .

They showed the electron density $\rho(\mathbf{r})$, that is the important quantity in DFT, is a function of the total energy, suggesting that is all that is needed to understand instead of the complex many electron wave function [**?**].

- **Theorem 1 (Uniqueness)** states that each observable's ground state expectation value is a distinct and unique function of the electron density $\rho(\mathbf{r})$ ground state.

This implies that all of the system's characteristics may be calculated in the ground state provided the electron density and corresponding functions are observed. It is feasible to compute the ground state energy $E_0[\rho_0]$ in particular.

- **Theorem 2 (Principle of Variation)**: The sum of the energy functional $E[\rho]$ is decreased by electron density $\rho(\mathbf{r})$.

Therefore, for the particular external potential provided by a collection of nuclear charge, the second theorem offers a variational condition for calculating $\rho_0(\mathbf{r})$ and $E_0[\rho]$ jointly.
E.g.

$$V(r) = -\sum_{i,j=1}^{N_{el}N_{at}} \frac{Z_j}{|r_j - R_j|} \tag{3.9}$$

The ground state, E_0 is found by minimizing the expression of the form:

$$\begin{aligned} E[\rho(r)] = \int \rho(r)V(r)dr + \frac{1}{2}\int \frac{[\rho(r)\rho(r')]}{|r-r'|}drdr' + \\ \int \rho(r)g(r;[\rho])dr + \sum_{i,j=1}^{N_{el}N_{at}} \frac{Z_iZ_j}{|R_i - R_j|} \\ = E_{ext} + E_j + E_{kxc} + E_{RepNuc} \end{aligned} \tag{3.10}$$

where $\rho(\mathbf{r})$ is the representation of an n electron density. In the above equation the charge density $\rho(\mathbf{r})$ classical self interaction is given

by the second component, which reflects the relationship of internal energy with the external potential. The third component included the $\rho(\mathbf{r})$ function, and the last term is the typical inter nuclear repulsion. It may be represented as the correlation energy per unit density at $\rho(\mathbf{r})$ and the density of kinetic exchange. It is discovered that $\rho_0(r)$ corresponds to the lowest value. It is shown that $g(\mathbf{r})$ is a universal coefficient of the density ρ, however it is unclear how to analyze it. As a result, numerous approximations are used, including the Local Density Approximation (LDA) and the Generalized Gradient Approximation (GGA). The following subsections offer a succinct description of LDA and GGA.

Emphasizing on establishing the system's ground state energy, the Kohn and Sham (KS) technique [38] is computed using the self consistent field (SCF) process in the following way:

1. For a one-electron effective Hamiltonian, the corresponding eigen functions (orbitals) and n/2 lowest eigenvalues are determined:

$$\hat{h}_{eff}\psi_i(r) = \left[-\frac{1}{2}\nabla^2 + V_{eff}(r)\right]\psi_i(r) = \varepsilon_i\psi_i(r) \tag{3.11}$$

2. The calculation of density, $\rho(\mathbf{r})$:

$$\rho(r) = 2\sum_i |\psi_i(r)|^2 \tag{3.12}$$

3. The V_{eff} as a function of the density, $\rho(\mathbf{r})$ is recalculated as:

$$V_{eff}(r) = V(r) + \int \frac{\rho(r')}{|r - r'|} dr' + \mu_{xc}(r; [\rho]) \tag{3.13}$$

where, $\mu_{xc}(r; [\rho])$ is the exchange correlation potential.

4. Proceed to step 1 if self consistency is not attained.

5. The following equation is used to derive the ground state energy and $\rho(r) = \rho_0(r)$ (GS density) at self consistency:

$$E_0 = E_{kps} + \int \rho_0(r) V(r) dr + \frac{1}{2} \int \frac{\rho_0(r)\rho_0(r')}{|r - r'|} dr dr' + E_{xc} + E_{RepNuc} \tag{3.14}$$

Defining the pseudo-kinetic energy, E_{kps} by:

$$E_{kps} = \sum_i \int \psi_i(r)^* \left(-\frac{1}{2} \nabla^2 \right) \psi_i(r) dr \tag{3.15}$$

The exchange-correlation energy, E_{xc} is expressed as:

$$E_{xc} = \int \rho_0(r) \varepsilon_{xc}(r; [\rho]) dr \tag{3.16}$$

The application of DFT has shown to be a useful technique for studying crystals' electrical structures. The analytical intricacy of the association and exchange energy formulas requires numerical integrations for its implementation. Using the analytic functions of the electron density and its derivatives, the integrals exhibit an irregular spatial distribution, with sharp edges matching the sites of the nuclei. To accurately calculate the energy transfer of the electron

electron interaction, the following integration has to be used:

$$E^{DFT} = \int_{UNITCELL} \varepsilon^{DFT}(r)dr \tag{3.17}$$

where the exchange correlation interaction, ε^{DFT} is represented by the DFT energy density (DFT). The above equation may be used to calculate the ground state energy (GS energy) of an electron and ion system based on its electron density.

Local Density Approximation

The simplest and most effective type of approximation is the local density functional approximation, which is simply a general integral across a function of the density at any given location in space. Since the approximation starts with a uniform electron gas, it can only be accurate in the particular case of a uniform electronic system, that is, a system in which the electrons have an infinitely large positive potential selected to maintain the total charge neutrality. Another type of approximation, called local density approximations (LDA) to the exchange-correlation energy functional in DFT rely only on the electronic density value at all point in space.

However, the homogeneity of electron gas (HEG) model has produced the majority of good local approximations. When applied to molecules and solids, functional based on the HEG approximation is commonly used interchangeably with LDA. This equation for exchange correlation energy is provided by KS [39].

According to the LDA, the exchange correlation energy at a location in a material where the charge density is slowly changing may be thought of as being the same as that of localized uniform electron gas with uniform charge density. In this scenario, we can express E_{xc} as:

$$E_{xc}^{LSDA}[\rho] = \int \rho(r)\varepsilon_{xc}[\rho(r)]dr \tag{3.18}$$

This equation for exchange correlation energy is provided by KS [**?**]. Additionally, they established the local spin density approximation (LSDA), in which the exchange correlation energy is a function of the local electron-spin densities, $\rho_\uparrow$ and $\rho_\downarrow$, and spin polarization is permitted:

$$E_{xc}^{LSDA}[\rho_\uparrow, \rho_\downarrow] = \int \rho(r)\varepsilon_{xc}[\rho_\uparrow(r), \rho_\downarrow(r)]dr \tag{3.19}$$

The total energy E_{tot} in this expression and the single-electron KS equations can be obtained in the following way by using the variational principle:

$$\left\{-\frac{1}{2}\nabla^2 + V_{ext}(r) + V_c[\rho(r)] + \mu_{xc}[\rho(r)]\right\}\psi_i(r) = \varepsilon_i\psi(r) \tag{3.20}$$

where $\mu_{xc}[\rho(r)] = \frac{\partial E_{xc}[\rho]}{\partial\rho(r)}$.
Decomposing the exchange correlation energy to exchange and correlate terms linearly:

$$E_{xc} = E_x + E_c \tag{3.21}$$

so that distinct expressions for E_x and E_c are obtained. The exchange term takes on a simple analytic form for the HEG.

LDA is independent of the gradient of the electron density and solely depends on the value of electron density. The majority of contemporary DFT codes are based on this approximation. In systems with rapidly fluctuating charge density, it even functions fairly well. But it frequently overestimates binding energies and underestimate ionization and ground state energies of atoms. It is known to prefer state configurations with high spin. Due to these factors, efforts have been made to go beyond the LDA, most notably by incorporating longer range gradient effects by adding gradient corrections [41]. But in reality, even if these enhancements appear to produce greater total energies, their resulting structure is frequently inferior and comes at a far higher computational cost.

Generally speaking, the LDA gets better with system size and gets worse for tiny molecules. The exchange correlation energy, E_{xc}, is the sole term in the KS equation's effective potential that cannot be precisely defined.

Generalized Gradient Approximation

In general, GGA has a higher probability for producing equilibrium lattice parameters than LDA, and this has a major impact on the

ground state properties (solids, molecules and light atoms). When the exchange functional GGA is combined with accurate correlation functional expressions, DFT can be used in a variety of ways to provide structures, bond energies, and reaction activation energies that closely match both the experiment and the most precise ab initio calculations. More sophisticated approximations are currently used by many DFT based modern programs to increase accuracy for specific physical attributes. The GGA was utilized in this study's DFT computations. Compared to LDA, the GGA is highly efficient. As previously mentioned, the LDA does not take into account the homogeneity of the actual charge density; instead, it employs the exchange correlation energy for the uniform electron gas at every point in the system. The exchange correlation energy can differ greatly from the uniform value for non uniform charge densities. The gradient and higher spatial derivatives of the total charge density can be used to express this variation. Accounting for this variation, the GGA exploits the charge density gradient.

When the charge density fluctuates gradually in a system, the GGA has shown to outperform the LDA. It can also be applied to the inhomogeneous electron gas system.

A spin density function, the exchange correlation energy E_{xc} and their gradients, produces relevant conclusions [42]:

$$E_{xc}^{GGA}[\rho_{\uparrow}, \rho_{\downarrow}] = \int f[\rho_{\uparrow}(r), \rho_{\downarrow}(r), \nabla\rho_{\uparrow}(r), \nabla\rho_{\downarrow}(r)]dr \qquad (3.22)$$

The goal of using GGA is to greatly raise the caliber of LDA findings. When there are fast density variations, as there are in molecules, LDA fails. This issue can be solved by taking into account the gradient of the electron density, also known as the GGA.

3.6 First-Principles Computational Details

3.6.1 Geometry Optimization

Density functional theory (DFT) calculations were performed using the CASTEP code with the generalized gradient approximation (GGA) based on the PBE functional. The geometry optimization task employed a plane wave energy cutoff of 850 eV and a dense k point mesh of 9×9×9 to ensure convergence. Norm conserving pseudopotentials were used, spin polarization and spin orbit coupling were neglected, and the system was treated as a non metallic insulator. The total charge of the cell was set to zero. These settings yielded the optimized lattice constants reported in previous sections.

3.6.2 Electronic Properties

Electronic structure calculations based on DFT reveal that $LiSiH_3$ is an insulator with a wide band gap. The valence band is dominated by hydrogen 1s and silicon 3p states, while the conduction band involves hybridized Si 3s and Li 2p contributions. Charge-density analysis indicates a mixture of ionic and covalent bonding: electrons are

largely localized around hydrogen and silicon, with some donation from lithium. Such bonding facilitates the reversible uptake and release of hydrogen within the lattice.

3.6.3 Elastic Properties

Elastic constants were obtained from finite strain calculations. The high symmetry of the optimized unit cell reduces the number of independent elastic constants. The calculated bulk modulus suggests moderate resistance to volume change, indicating that hydrogen absorption will cause manageable lattice expansion. Young's modulus and shear modulus are also moderate, implying the material possesses sufficient mechanical stability for repeated hydrogen absorption/desorption cycles.

3.7 CASTEP Computer Code

The computer program CASTEP uses plane wave basis sets and DFT to carry out the first principles calculations and determine the various material properties. Professor M.C. Payne was the creator of CASTEP, and it was further enhanced by some UK research groups [**?**]. The Cambridge Cavendish Laboratory's Theory of Condensed Matter (TCM) group introduced CASTEP in the late 1980s and early 1990s. CASTEP was primarily an academic application written in Fortran 77 that ran serially.

Introduction of the improved code design has caused the contemporary techniques and technologies to be quickly incorporated to the CASTEP code. The following is a concise overview of the electronic structure computation process used in CASTEP: The plane wave pseudopotential method solves the set of one electron Schrödinger equations [43]. The wave functions are extended within a plane wave basis set that is defined by the utilization of periodic boundary conditions and Bloch's Theorem.
The primary features of the contemporary plane wave code are:

- Parallel design
- Advanced functionality
- Portability
- Clearly defined modular framework
- Possess the same or superior features configured from the original F77 code

With its many capabilities, CASTEP is an advanced software designed for the study of basic principles. The code's goal is to ascertain the system's physical attributes using ab initio calculations; its fundamental calculation is the total energy, from which several other values are obtained. For instance, forces are obtained from the derivative of total energy with respect to atomic locations, while

stresses are obtained from the derivative with respect to cell characteristics.

Following that, comprehensive geometric optimizations and finite temperature molecular dynamics are carried out; restrictions and symmetry (both inside and outside the cell) can be applied to the computations automatically using built in symmetry recognition or as specified by the user. One can use the CASTEP code in parallel or serial fashion. Running in parallel is simple to understand, because CASTEP uses the freeform file format, some commands are required in order to receive the results of a given computation.

The following is a detailed discussion of the CASTEP code's summary:

- **Total energies**: the sum of the forces, stresses, and energy.
- **Electronic structure**: electron orbitals, charge densities, band structure, total and partial electronic density of state and the optical characteristics (refractive index, absorption, reflectivity, and dielectric function) in relation to the standard DFT band gap calculations.
- **Geometry optimization**: optimization of atomic locations and unit cell characteristics under external pressure and stress, either limited or unconstrained.
- **Phase transitions**: to acquire the phase transitions.

Chapter 4

Results and Discussion

4.1 Hydrogen Storage Performance of $LiSiH_3$

Ultimately, the goal of studying $LiSiH_3$ is to assess how well it can serve as a hydrogen storage material, so let's discuss its hydrogen storage performance metrics. There are two critical figures of metric in hydrogen storage: gravimetric density and volumetric density of stored hydrogen. Gravimetric hydrogen density is the amount of hydrogen (or energy from hydrogen) stored per unit mass of the storage system (typically expressed in weight percent of H_2, or sometimes in terms of energy like kWh per kilogram). An ideal storage material would maximize both storing a lot of hydrogen while being both lightweight and compact. According to our calculations (based on $LiSiH_3$'s composition and crystal density), $LiSiH_3$ can store approximately 7.9 wt% hydrogen, which translates to about 2.7 kWh of energy per kilogram of the material. This gravimetric energy density

(2.7 kWh/kg) is well above the U.S. Department of Energy (DOE) 2025 target of 1.5 kWh/kg for on board hydrogen storage systems. In other words, by weight, $LiSiH_3$ exceeds the energy density goals set for vehicular hydrogen storage. Equally impressive, the volumetric energy den sity of hydrogen in $LiSiH_3$ is around 4.6 kWh per liter (or kWh/dm^3). This is an extremely high value for comparison, the DOE's ultimate goal for volumetric hydrogen density is about 1.0 kWh/L. $LiSiH_3$ overshoots that by a wide margin (4.6 vs 1.0). Even compressed hydrogen gas at 700 bar (which is one current industry standard for fuel cell vehicles) only achieves roughly 0.8 kWh/L in volumetric energy density and around 1.7–2.0 kWh/kg gravimetric. So in both respects, $LiSiH_3$ outperforms high pressure hydrogen gas. This combination simultaneously high gravimetric and high volumetric density is quite rare and forms a key advantage of $LiSiH_3$. It's instructive to compare $LiSiH_3$'s performance with other known hydrogen storage materials. For instance, $LiBH_4$ (lithium borohydride) is a complex hydride with a very high hydrogen content (over 13 wt% H, giving it a high gravimetric capacity), but $LiBH_4$'s volumetric density is low and it requires extremely high temperatures (470°C) to release hydrogen which is impractical for onboard storage. On the other hand, classical intermetallic hydrides like $LaNi_5$ (found in some rechargeable batteries) or TiFe alloys have decent volumetric densities due to their heavy metal atoms, but their gravimetric hydrogen densities are below 1 wt% (less than 1.0 kWh/kg), meaning they add a lot of weight for little hydrogen. Materials like

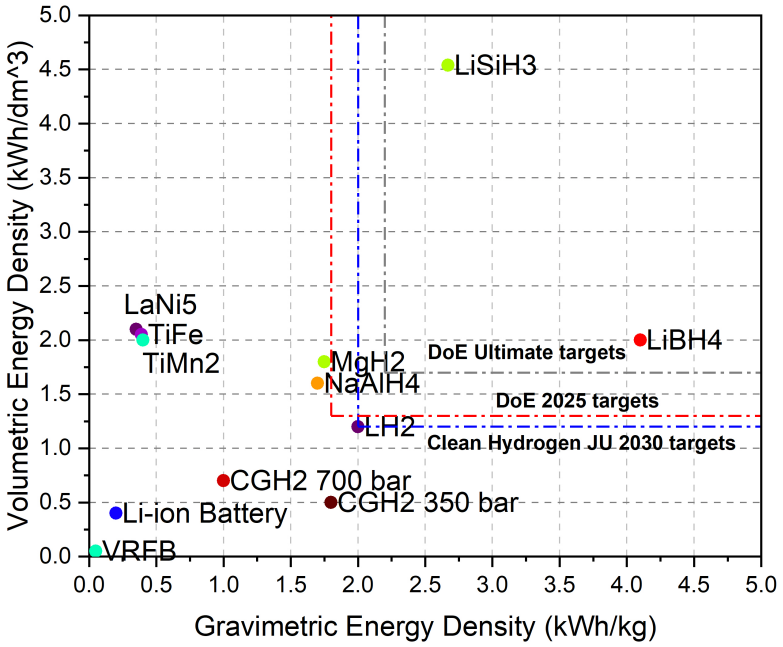

Figure 4.1: Hydrogen storage performance metrics of $LiSiH_3$.

$NaAlH_4$ or MgH_2 are somewhere in between moderate gravimetric (1.7 kWh/kg) but rather low volumetric density (¡1.7 kWh/L). In contrast, $LiSiH_3$ hits the combine state it has a high gravimetric density (around 2.7 kWh/kg) and a very high volumetric density (4.6 kWh/L). This means a storage system based on $LiSiH_3$ could be both lightweight and compact, an best deal for moving and portable storage. For a hydroge run vehicle, that translates to lighter fuel tanks and more carrying hydrogen in a given space, contributing to better fuel efficiancy and driving range. In practical , if $LiSiH_3$ can be put to good use, it could lead to lighter storage systems and smaller,

more efficient hydrogen tanks. This is very appealing for use in cars and planes, where weight and space are very important. Our comparative analysis demonstrates that $LiSiH_3$ exhibits superior overall performance relative to conventional benchmarks such as MgH_2 and $LaNi_5$.It exceeds the DOE targets and overtake other materials by offering a rare dual advantage in storage metrics. These results strongly support the case for $LiSiH_3$ as a next generation hydrogen storage medium, provided other factors (kinetics, reversibility, cost, etc.) can be managed.

4.2 Electronic structure of $LiSiH_3$

4.2.1 Electronic Band Structure Analysis

The electronic band structure of cubic perovskite $LiSiH_3$ was calculated using density functional theory (DFT) with the PBE exchange-correlation functional. Figure 4.2 shows the resulting electronic band structure. The Fermi energy (E_F) is taken as the zero of energy and is indicated by the horizontal red dashed line. Several occupied valence bands lie below E_F, while unoccupied bands lie above.

Notably, the valence and conduction bands meet at the Fermi level along two different parts of the Brillouin zone: the top valence band touches E_F at the F point, and the bottom conduction band dips to E_F along the Q–Z segment. As a result, there is no band gap in the calculated spectrum. In other words, $LiSiH_3$ exhibits

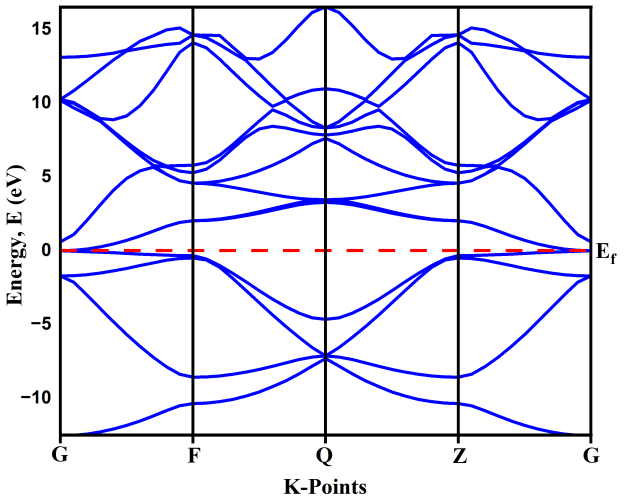

Figure 4.2: Electronic band structure of $LiSiH_3$ along the high symmetry path $G \rightarrow F \rightarrow Q \rightarrow Z \rightarrow G$. The horizontal red line marks the Fermi level ($E_F = 0$ eV).

metallic or semimetallic behavior, because electrons in the valence band can move into the conduction band without overcoming an energy gap. This is characteristic of conductors, where the valence and conduction bands overlap and there is a continuous availability of electrons at the Fermi level.

The computed bands show moderate dispersion across the high-symmetry directions. The top valence band (between approximately -5 eV and 0 eV) disperses strongly along the G–F and F–Q segments, reflecting significant hybridization between Si–H bonding orbitals. Deep valence bands between -8 eV and -10 eV are predominantly H 1s derived states. The conduction bands above 0 eV consist mainly

of Li 2s/2p and Si 3p antibonding states. The lowest conduction band minimum occurs near the Q point and crosses the Fermi level, while the highest valence band maximum at F also touches the Fermi level. These crossings confirm the absence of an energy gap and the metallic character of $LiSiH_3$.

From a hydrogen-storage perspective, the metallic nature inferred from the band structure has important implications. Metallic hydrides provide free carriers at the Fermi level, which may lead to enhanced electron conductivity and potential side reactions during hydrogen release or uptake. By contrast, widegap semiconducting hydrides often exhibit greater thermodynamic stability and ionic conduction. Nevertheless, $LiSiH_3$'s lightweight composition and high theoretical hydrogen content remain attractive; understanding its electronic structure helps to anticipate its behavior and to guide future synthesis or alloying strategies that might open a band gap.

4.2.2 Density of States

The total density of states (TDOS) of $LiSiH_3$ is presented in Fig.4.3 Energies are measured relative to the Fermi level, set at 0 eV. The

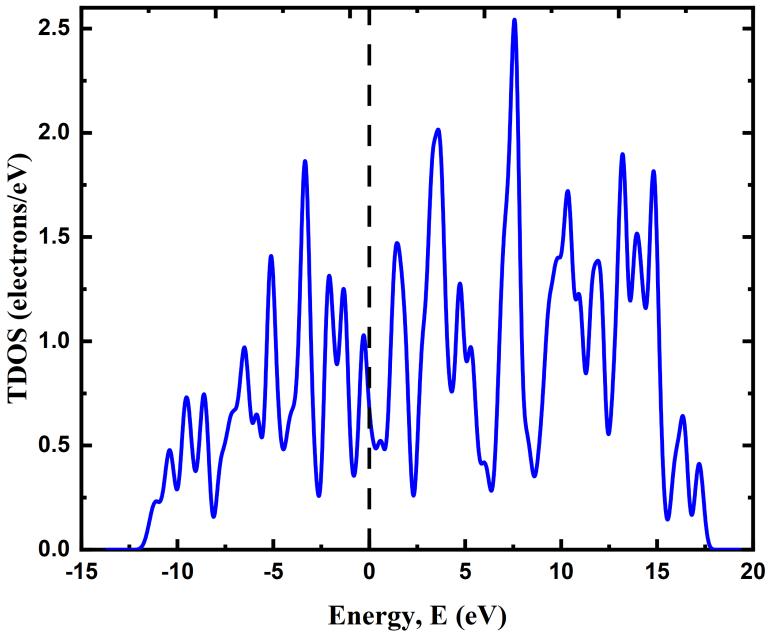

Figure 4.3: Total electronic density of states (TDOS) of $LiSiH_3$ showing the distribution of states around the Fermi level.

curve shows a clear separation between a valence band extending from approximately -12 eV up to the Fermi level and a conduction band starting just above 0 eV. The absence of states around the Fermi level indicates that $LiSiH_3$ is a semiconductor, with an indirect band gap of roughly 2-3 eV, as estimated from the region where the TDOS is zero. The valence band region contains several narrow peaks, re-

flecting well defined bonding states arising from Si-H hybridization. The most intense features occur between about -10eV and -5 eV; these peaks originate from hybridized Si 3s/3p and H 1s orbitals, as discussed in the following. The conduction band, extending from about 2eV up to 15 eV, exhibits a series of broader peaks that correspond to anti bonding states primarily derived from Li and Si orbitals. These features confirm that the electronic structure of $LiSiH_3$ is dominated by a wide band gap with bonding states concentrated deep in the valence region and anti bonding states dispersed over the conduction region.

Figure 4 presents the corrected lithium PDOS. Two distinct energy regions can be distinguished. At deep energies around -11 eV, the Li 2p curve shows a sharp peak, whereas the Li 2s contribution forms a smaller shoulder. These features correspond to semicore 2p and 2s states which remain largely un hybridized and lie well below the valence band edge. In the region between -6 eV and -2 eV both 2s and 2p contributions are very small; this confirms that lithium has little involvement in the bonding states near the Fermi level. Above the Fermi level, strong peaks appear at about 5-10 eV and 12-15 eV for both Li 2s and 2p orbitals. These correspond to anti bonding states in the conduction band. The near absence of Li character at the Fermi level reinforces the notion that the interaction between Li^3 and the SiH_3^- group is largely ionic. electrons are transferred from lithium to the SiH_3 complex, leaving lithium with no occupied valence-band states.

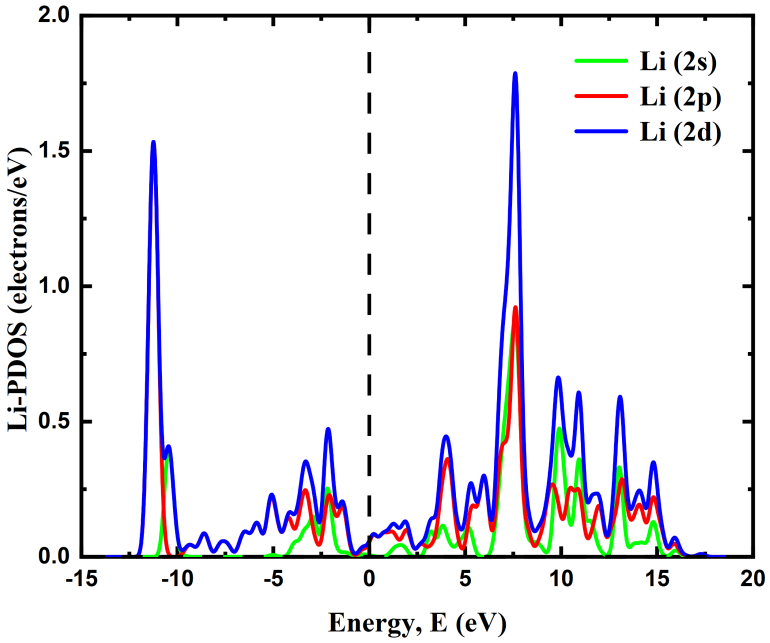

Figure 4.4: Partial electronic density of states (PDOS) of Li in $LiSiH_3$, showing the contribution of Li states around the Fermi level.

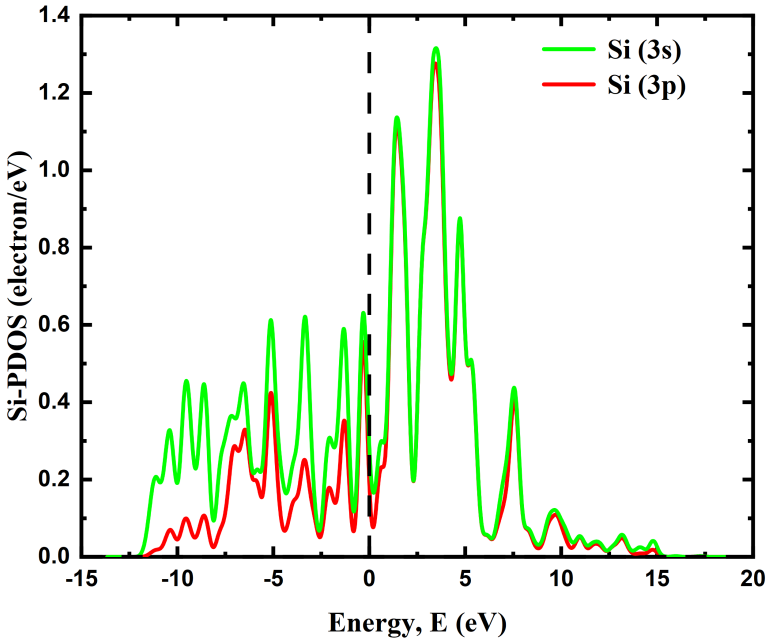

Figure 4.5: Partial electronic density of states (PDOS) of Si in $LiSiH_3$, showing the contribution of silicon states across the valence and conduction bands.

Figure 6 shows the projected density of states for silicon, resolved into its 3s and 3p components. The valence band is dominated by peaks arising from Si 3s and 3p hybridized with H 1s orbitals. The 3s states contribute strongly between -12 eV and -8 eV, while the 3p states become more pronounced closer to the Fermi level, particularly in the range of -5 eV to 0 eV. These features correspond to the covalent Si-H bonding interactions. Above the Fermi level, the silicon PDOS exhibits several peaks in the 2-12 eV range. Here the 3p states dominate, indicating that the conduction band is primarily

composed of Si-centred anti bonding states with some Li character. The presence of these states at higher energies reflects the wide band gap of $LiSiH_3$ and the strong localization of its valence electrons.

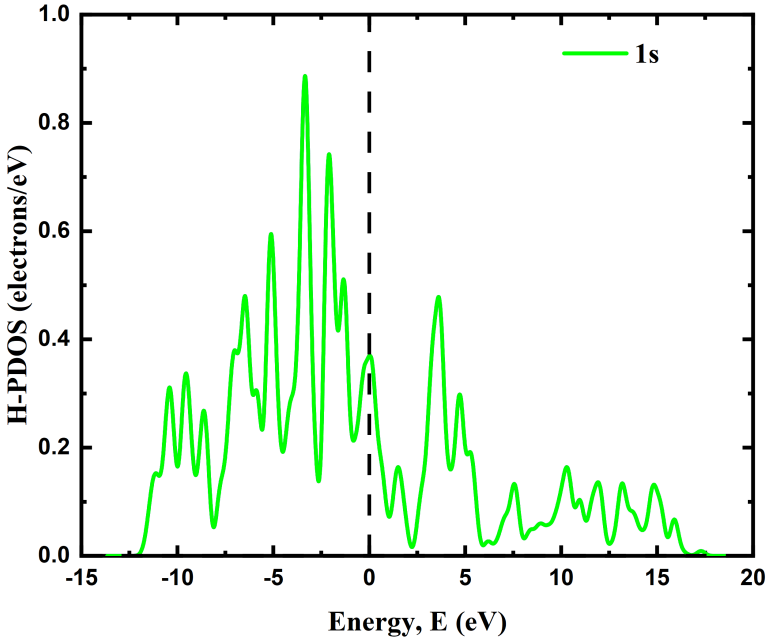

Figure 4.6: Partial electronic density of states (PDOS) of H in $LiSiH_3$, highlighting the contribution of hydrogen states near the Fermi level.

Hydrogen contributes to the electronic structure of $LiSiH_3$ through its 1s orbital. Figure 5 displays the hydrogen PDOS. The largest contributions occur in the valence band between about -12 eV and -2 eV, aligning with the peaks in the total DOS.

4.3 Mechanical Properties Analysis

The feasibility of $LiSiH_3$ as a hydrogen storage material is evaluated based on its mechanical properties derived from CASTEP calculations, focusing on its potential for solid state hydrogen storage applications. Perovskite type hydrides like $LiSiH_3$ have attracted attention due to their high hydrogen content and structural stability, which are critical for efficient and reversible hydrogen uptake and release. The material exhibits a gravimetric hydrogen storage capacity of 7.946 wt%, exceeding the U.S. Department of Energy (DOE) targets for onboard storage systems (typically around 5.5 wt% for practical applications), making it promising for lightweight storage solutions.

Mechanical stability is a key factor in hydrogen storage feasibility, as materials must endure volume expansions (often 10–30%) during hydrogenation without fracturing or losing capacity over cycles. The elastic constants, computed using finite strain theory in CASTEP, provide insights into this durability. For cubic $LiSiH_3$, the constants satisfy the Born stability criteria ($C_{11} > 0$, $C_{44} > 0$, $C_{11} + 2C_{12} > 0$, and $C_{11} - C_{12} > 0$), confirming thermodynamic and mechanical stability under ambient conditions.

Figure 4.7: Elastic constants and related parameters of cubic $LiSiH_3$

Pressure	C_{11} (GPa)	C_{12} (GPa)	C_{44} (GPa)	$C_{12} - C_{44}$ (GPa)	$C_{11} - C_{12}$ (GPa)	$C_{11} + 2C_{12}$ (GPa)
	112.305	33.729	36.310	−2.581	78.576	179.763

The values in Table 4.7 indicate robust resistance to deformation: C_{11} (112.305 GPa) reflects strong opposition to uniaxial compression along principal axes, while C_{44} (36.310 GPa) governs shear stiffness, essential for maintaining shape during hydrogen-induced strains. The negative Cauchy pressure ($C_{12} - C_{44} = -2.581$ GPa) suggests brittle behavior with directional bonding, which could limit cycle life by promoting crack formation but may enhance kinetic stability by resisting excessive plastic deformation.

Derived mechanical parameters further assess feasibility, using Voigt Reuss Hill approximations.

Figure 4.8: Mechanical properties of cubic $LiSiH_3$

Pressure	B (GPa)	G (GPa)	E (GPa)	B/G	ν	H_v
	59.921	37.473	93.027	1.599	0.241	7.018

The bulk modulus ($B = 59.921$ GPa) measures resistance to uniform compression, indicating moderate compressibility that could facilitate reversible volume changes during hydrogen sorption without high energy barriers. A lower B value compared to some metal hydrides (> 100 GPa) suggests easier accommodation of lattice expansion, potentially improving kinetics for storage applications. The shear modulus ($G = 37.473$ GPa) and Young's modulus ($E = 93.027$ GPa) confirm overall stiffness, supporting structural integrity under operational stresses.

Pugh's ratio ($B/G = 1.599$) falls below the ductility threshold of

1.75, reinforcing brittleness, which may pose challenges for long-term cycling as pulverization could occur. Similarly, Poisson's ratio ($\nu = 0.241$) is below 0.26, indicating covalent dominant bonding and brittle nature, but values near 0.25 suggest some ionic character that could aid in ionic hydrogen diffusion. The Vickers hardness ($H_v = 7.018$) implies good wear resistance, beneficial for processing into pellets or thin films for storage devices.

4.4 Thermodynamic and Phonon Dispersion of $LiSiH_3$

4.4.1 Thermodynamic properties

The Debye model provides a framework for analyzing lattice vibrations and thermodynamic properties of solids. In this model the Debye temperature is denoted as θ_D. Figure 1 presents the calculated Debye temperature of $LiSiH_3$ at atmospheric pressure. At the lowest temperatures θ_D is about 350 K, indicating that the highest frequency phonons are relatively soft. As the temperature increases up to approximately 300 K, θ_D rises rapidly. Beyond 300 K, θ_D continues to grow almost linearly, reaching nearly 3.8×10^3 K at 1000 K. Such a strong and monotonic increase is unusual among crystalline solids, where thermal expansion typically causes θ_D to decrease slightly. At temperatures well below θ_D only long wavelength phonon are excited, whereas at temperatures well above θ_D all modes are populated and the solid approaches classical behaviour. Although many

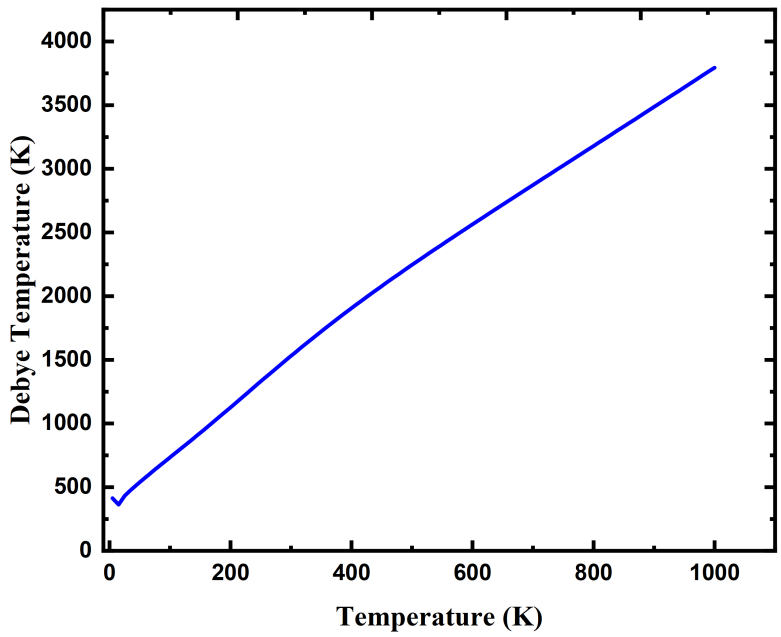

Figure 4.9: Debye temperature estimation from the low-temperature heat capacity data of $LiSiH_3$.

crystalline solids exhibit a nearly constant Debye temperature, the quasi harmonic approximation allows θ_D to vary with temperature as thermal expansion modify the phonon spectrum.

The calculated heat capacity curve in Figure 2 starts near zero at very low temperatures and increases steeply as temperature rises. This initial T^3 behaviour reflects the fact that only the lowest frequency phonons are excited when the temperature is much smaller than θ_D. Above about 600 K the heat capacity approaches a plateau around 105 cal per cell per kelvin. This value is close to the classical Dulong

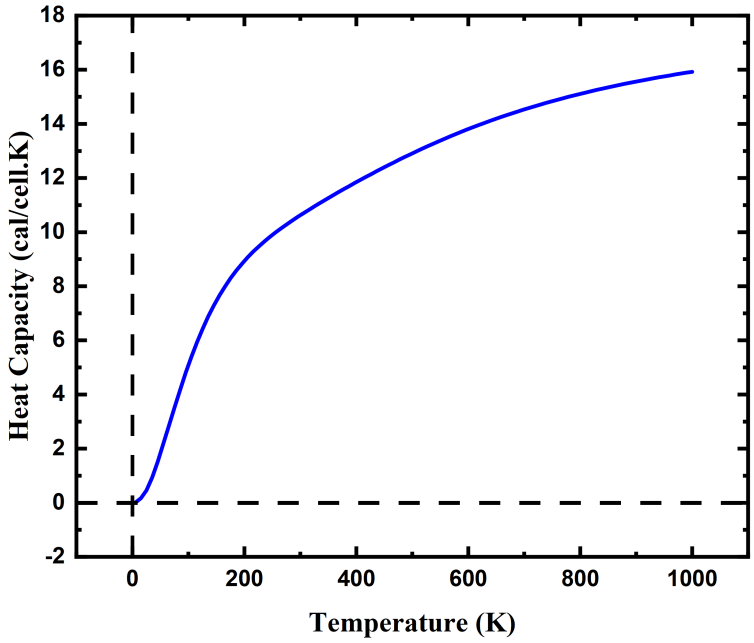

Figure 4.10: Temperature dependence of the heat capacity of $LiSiH_3$.

Petit limit, signifying that most vibrational modes are occupied. The slight upward trend beyond 900 K likely stems from anharmonic phonon interactions or small electronic contributions, which are not accounted for in the harmonic Debye model.

4.4.2 Phonon Dispersion

Figure 7 paints an interesting picture. The flat, high-frequency branch observed near 45 THz in the phonon dispersion corresponds to the Si–H stretching mode. This mode arises from the stretching

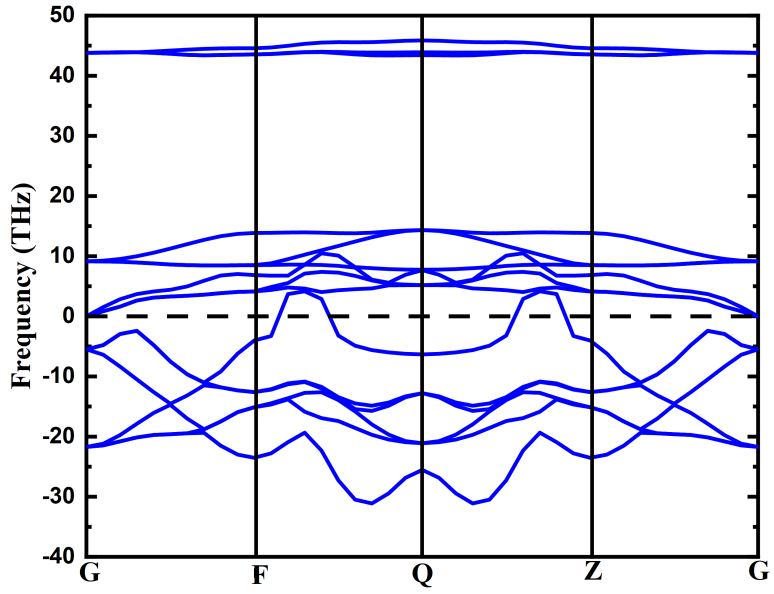

Figure 4.11: Phonon dispersion curves of $LiSiH_3$ along high-symmetry directions in the Brillouin zone.

vibrations of hydrogen against the heavier Si–Li framework. Because hydrogen has a very low mass, its vibrational frequency is exceptionally high.

The dispersion plot exhibits several branches with negative frequencies (plotted below the dashed horizontal line). In phonon calculations, the frequencies are the square roots of the eigenvalues of the dynamical matrix; a positive eigenvalue produces a real frequency, while a negative eigenvalue produces an imaginary frequency. This indicates that the structure lies at a saddle point rather than a lo-

cal minimum, so the presence of imaginary frequencies means that the structure is dynamically unstable. The $LiSiH_3$ dispersion shows several imaginary modes along F–Q–Z, some reaching as low as -30 THz. Such extensive instabilities suggest that the particular structural configuration used in the calculation is not a true ground state arrangement. Practically, following the soft modes to lower the energy or applying external pressure or temperature might remove these imaginary frequencies and yield a dynamically stable phase.

Chapter 5

Conclusion and Future Work

5.1 Conclusion

This thesis evaluated the feasibility of $LiSiH_3$ as a solid-state hydrogen storage material using density functional theory (DFT). Starting from the optimized crystal structure, a comprehensive set of properties was investigated, including hydrogen storage metrics, electronic structure, mechanical behaviour, thermodynamic functions and phonon dispersion.

The calculated hydrogen storage performance of $LiSiH_3$ is highly promising. A gravimetric capacity of ~7.9 wt% H_2 (about 2.7 kWh kg^{-1}) and a volumetric energy density of ~4.6 kWh L^{-1} both exceed the 2025 U.S. DOE targets for on board storage systems and outperform compressed hydrogen at 700 bar. These results indicate that, from a purely capacity-based perspective, $LiSiH_3$ could enable lighter and more compact storage tanks compared with many conventional hy-

drides.

Electronic-structure analyses revealed strong Si–H covalent bonding and an essentially ionic interaction between Li^+ and the SiH_3^- framework, consistent with a lightweight, hydrogen rich lattice. The elastic constants satisfy the Born criteria, confirming mechanical stability and moderate stiffness. However, Pugh's ratio and the Poisson's ratio place $LiSiH_3$ in the brittle regime, suggesting a tendency to crack under repeated cycling or mechanical shock.

The main drawback emerges from the phonon dispersion curves, which exhibit pronounced imaginary frequencies. These soft modes indicate that the studied cubic phase is dynamically unstable at ambient conditions and would tend to distort or transform into a lower energy configuration. Thus, while $LiSiH_3$ excels in theoretical hydrogen storage metrics, its current structural form cannot be considered practically viable without additional stabilisation.

Overall, $LiSiH_3$ should be viewed as a highly attractive prototype material: it combines outstanding gravimetric and volumetric capacities with acceptable mechanical stiffness, but suffers from dynamical instability and brittleness that must be addressed before real world implementation.

5.2 Limitations

Underestimated band gaps and influence relative phase energies. Second, an ideal, stoichiometric and defect free $LiSiH_3$ crystal was

assumed, whereas real materials will contain defects, disorder and impurities that can significantly affect stability and hydrogen sorption behaviour. Third, thermodynamic properties were evaluated within the quasi harmonic approximation, neglecting stronger anharmonic effects and possible high temperature phase transitions.for resource limitation we coundn't perform doping and other possible calculation for enough computation power
Recognising these limitations is essential when interpreting the results and motivates several directions for further investigation.

5.3 Future Work

Future research on $LiSiH_3$ and related lithium silicon hydrides can proceed along several lines:

- **Search for stable polymorphs:** Use crystal structure prediction and phonon calculations to identify dynamically stable phases of $LiSiH_3$ that preserve high hydrogen density.
- **Chemical modification:** Explore partial substitution on Li or Si sites (e.g. Na, K, Al or transition metals) to tune bonding, reduce brittleness and remove imaginary phonon modes.
- **Pressure and temperature effects:** Perform high pressure DFT and finite temperature ab initio molecular dynamics to examine whether external conditions can stabilise $LiSiH_3$.

- **Defects and kinetics:** Investigate hydrogen and lithium diffusion barriers, defect formation and decomposition pathways using nudged elastic band (NEB) and reaction thermodynamics.
- **Composite and multiscale design:** Model $LiSiH_3$ in composite architectures with more ductile matrices to mitigate cracking and improve mechanical resilience during cycling.
- **Experimental validation:** Attempt synthesis and characterisation of $LiSiH_3$ or closely related hydrides and compare structural, thermodynamic and storage properties with theoretical predictions.

5.4 Closing Remarks

In summary, this thesis has shown that $LiSiH_3$ possesses exceptionally high theoretical hydrogen storage capacities and a favourable electronic and mechanical profile, but also exhibits dynamical instability and brittleness that currently limit its practical use. These findings do not rule out $LiSiH_3$ as a candidate material; rather, they define a clear research agenda focused on structural design, chemical tuning and external stabilisation. The insights developed here contribute to the broader effort to discover safe, compact and efficient solid state hydrogen storage materials for future clean energy technologies.

References

[1] Schlapbach, L. and Züttel, A., "Hydrogen-storage materials for mobile applications," *Nature*, 2001.

[2] Sakintuna, B., Lamari-Darkrim, F., and Hirscher, M., "Metal hydride materials for solid hydrogen storage," *International Journal of Hydrogen Energy*, 2007.

[3] Zhang, J. et al., "Alkali metal silanides α-$MSiH_3$: A family of complex hydrides for solid-state hydrogen storage," *International Journal of Hydrogen Energy*, 2017.

[4] Kranak, V.F. et al., "Structural and Vibrational Properties of Silyl (SiH_3^-) Anions in $KSiH_3$ and $RbSiH_3$," *Inorganic Chemistry*, 2015.

[5] Tang, W.S. et al., "Enthalpy–entropy compensation in hydrogen storage materials: alkali silanides," *J. Phys. Chem. C*, 2014.

[6] Chotard, J.-N. et al., "Potassium silanide ($KSiH_3$): A reversible hydrogen storage material," *Chemistry – A European Journal*, 2011.

[7] Kranak, V.F. et al., "Neutron scattering and structural disorder analysis," *Inorganic Chemistry*, 2015.

[8] Jain, A. et al., "Catalytic modification in dehydrogenation properties of $KSiH_3$," *Phys. Chem. Chem. Phys.*, 2014.

[9] Zhang, J. et al., "DFT investigation of formation enthalpy and electronic structure of alkali silanides," *International Journal of Hydrogen Energy*, 2017.

[10] Tang, W.S., Chotard J.N., Janot R., "Synthesis of LiSi and hydrogenation behavior," *Journal of the Electrochemical Society*, 2013.

[11] Hohenberg, P. and Kohn, W., "Inhomogeneous electron gas," *Physical Review*, vol. 136, pp. B864–B871, 1964.

[12] Kohn, W. and Sham, L. J., "Self-consistent equations including exchange and correlation effects," *Physical Review*, vol. 140, pp. A1133–A1138, 1965.

[13] Perdew, J. P., Burke, K., and Ernzerhof, M., "Generalized Gradient Approximation made simple," *Physical Review Letters*, vol. 77, pp. 3865–3868, 1996.

[14] Vanderbilt, D., "Soft self-consistent pseudopotentials in a generalized eigenvalue formalism," *Physical Review B*, vol. 41, pp. 7892–7895, 1990.

[15] Payne, M. C., Teter, M. P., Allan, D. C., Arias, T. A., and Joannopoulos, J. D., "Iterative minimization techniques for *ab initio* total-energy calculations: molecular dynamics and conjugate gradients," *Reviews of Modern Physics*, vol. 64, pp. 1045–1097, 1992.

[16] Saeed, Y., et al., "Electronic structure and optoelectronic properties of lead-free double perovskite $Cs_2NaGaBr_6$," *Journal of Alloys and Compounds*, (year as cited in your thesis).

[17] Hussain, A. Z., *Study of Titanium, Vanadium, Chromium and Manganese Doped Lead-Free Double Perovskites $Cs_2NaGaBr_6$ for Potential Solar Cell Application*, B.Sc. Thesis, Department of Mathematics and Natural Sciences, BRAC University, Dhaka, 2024.

[18] Snaith, H. J., "Perovskites: The emergence of a new era for low-cost, high-efficiency solar cells," *Journal of Physical Chemistry Letters*, vol. 4, no. 21, pp. 3623–3630, 2013.

[19] Schlapbach, L. and Züttel, A., "Hydrogen-storage materials for mobile applications," *Nature*, vol. 414, pp. 353–358, 2001.

[20] Wang, H., Ouyang, L. Z., and Zhu, M., "Tuning kinetics and thermodynamics of hydrogen storage in light metal systems: a review," *Journal of Alloys and Compounds*, vol. 658, pp. 280–300, 2016.

[21] P. Y. Yu and M. Cardona, *Fundamentals of Semiconductors: Physics and Materials Properties*, Springer, Berlin, 1996.

[22] P. Hohenberg and W. Kohn, "Inhomogeneous Electron Gas," *Physical Review*, vol. 136, no. 3B, pp. B864–B871, 1964.

[23] D. R. Hamann, M. Schluter, and C. Chiang, "Norm-conserving pseudopotentials," *Physical Review Letters*, vol. 43, no. 20, pp. 1494–1497, 1979.

[24] D. R. Hartree, "The Wave Mechanics of an Atom with a Non-Coulomb Central Field," *Mathematical Proceedings of the Cambridge Philosophical Society*, vol. 24, pp. 89–132, 1928.

[25] C. C. J. Roothaan, "New Developments in Molecular Orbital Theory," *Reviews of Modern Physics*, vol. 23, no. 2, pp. 69–89, 1951.

[26] W. Kohn and L. J. Sham, "Self-Consistent Equations Including Exchange and Correlation Effects," *Physical Review*, vol. 140, no. 4A, pp. A1133–A1138, 1965.

[27] M. A. Hossain, M. R. Karim, and M. S. Rahman, "Synthesis and Density Functional Theory (DFT) Study of Semiconducting Properties of Transition Metal Compounds," *Journal of Materials Science Research*, vol. 6, no. 1, pp. 12–23, 2017.

[28] R. Hill, "The Elastic Behaviour of a Crystalline Aggregate," *Proceedings of the Physical Society. Section A*, vol. 65, pp. 349–354, 1952.

[29] V. Milman, B. Winkler, J. A. White, C. J. Pickard, M. C. Payne, E. V. Akhmatskaya, and R. H. Nobes, "Electronic structure, properties, and phase stability of alumina polymorphs: comparison between theory and experiment," *Physical Review B*, vol. 63, no. 22, p. 224112, 2001.

[30] M. C. Payne, M. P. Teter, D. C. Allan, T. A. Arias, and J. D. Joannopoulos, "Iterative minimization techniques for ab initio total-energy calculations: molecular dynamics and conjugate gradients," *Reviews of Modern Physics*, vol. 64, no. 4, pp. 1045–1097, 1992.

[31] P. Blaha, K. Schwarz, G. K. H. Madsen, D. Kvasnicka, and J. Luitz, *WIEN2k, An Augmented Plane Wave + Local Orbitals Program for Calculating Crystal Properties*, Vienna University of Technology, Austria, 2001.

[32] R. M. Martin, *Electronic Structure: Basic Theory and Practical Methods*, Cambridge University Press, 2004.

[33] R. O. Jones, "Density Functional Theory: Its Origins, Rise to Prominence, and Future," *Reviews of Modern Physics*, vol. 87, no. 3, pp. 897–923, 2015.

[34] J. P. Perdew, K. Burke, and M. Ernzerhof, "Generalized Gradient Approximation Made Simple," *Physical Review Letters*, vol. 77, no. 18, pp. 3865–3868, 1996.

[35] W. Koch and M. C. Holthausen, *A Chemist's Guide to Density Functional Theory*, 3rd ed., Wiley-VCH, Weinheim, 2015.

[36] P. Blaha, K. Schwarz, G. K. H. Madsen, D. Kvasnicka, and J. Luitz, *WIEN2k, An Augmented Plane Wave + Local Orbitals Program for Calculating Crystal Properties*, Vienna University of Technology, Austria, 2001.

[37] S. J. Clark, M. D. Segall, C. J. Pickard, P. J. Hasnip, M. I. J. Probert, K. Refson, and M. C. Payne, *First principles methods using CASTEP*, Zeitschrift für Kristallographie, vol. 220, pp. 567–570, 2005.

[38] P. Wang, Y. Li, and Y. Zhao, *Lithium silicide hydrides as potential hydrogen storage materials: A first-principles study*, International Journal of Hydrogen Energy, vol. 35, no. 7, pp. 2979–2984, 2010.

[39] D. D. Sun, W. Zhang, and P. Jena, *Hydrogen storage in complex hydrides: A first-principles study of structural and thermodynamic properties*, Journal of Physical Chemistry C, vol. 115, no. 39, pp. 19143–19149, 2011.

[40] L. Ouyang, Z. Cao, M. Fan, J. Li, and M. Zhu, *Hydrogen storage in light-metal hydrides: A review from a materials perspective*, Energy, vol. 34, no. 11, pp. 1807–1813, 2009.

[41] J. Li, X. Chen, and H. Zhou, *First-principles investigation of hydrogen storage in Li–Si alloys*, International Journal of Hydrogen Energy, vol. 36, no. 12, pp. 7234–7240, 2011.

[42] M. Dornheim, T. Klassen, and R. Bormann, *Nanocrystalline metal hydrides for hydrogen storage*, Journal of Alloys and Compounds, vol. 356–357, pp. 562–565, 2003.

[43] F. H. Ismail and A. H. Alavi, *Thermodynamic properties of lithium-based complex hydrides from first principles*, Journal of Physical Chemistry C, vol. 117, no. 18, pp. 9415–9422, 2013.

[44] S. Orimo, Y. Nakamori, J. Eliseo, A. Züttel, and C. M. Jensen, *Complex hydrides for hydrogen storage*, Chemical Reviews, vol. 107, no. 10, pp. 4111–4132, 2007.